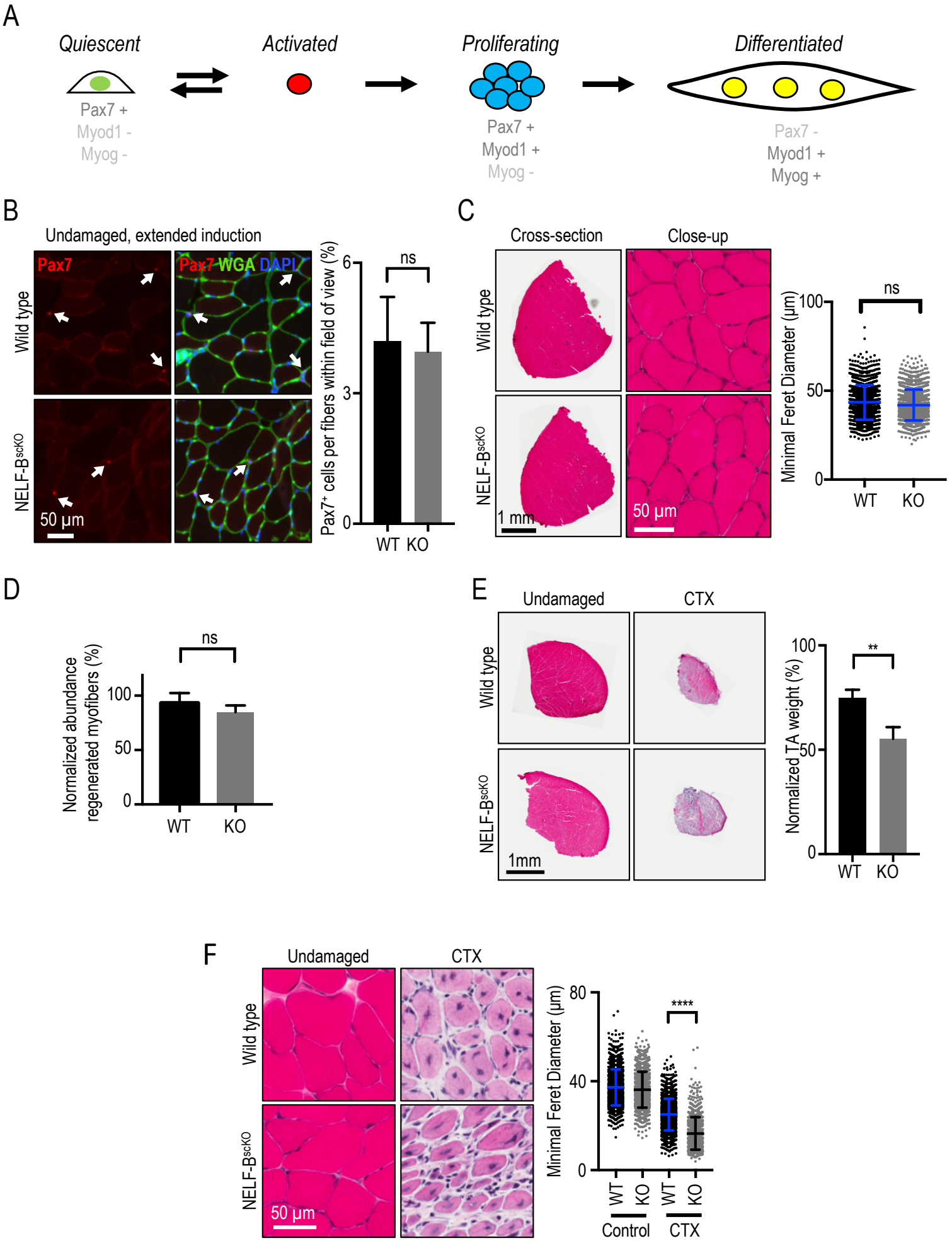
A
Quiescent
Activated
Proliferating
Differentiated
Pax7 +
Myod1 -
Myog -
Pax7 +
Myod1 +
Myog -
Pax7 -
Myod1 +
Myog +
B
Undamaged, extended induction
Pax7
Pax7 WGA DAPI
Wild type
NELF-BscKO
50 µm
Pax7+ cells per fibers within field of view (%)
ns
WT KO
C
Cross-section
Close-up
Wild type
NELF-BscKO
1 mm
50 µm
Minimal Feret Diameter (µm)
ns
WT KO
D
Normalized abundance regenerated myofibers (%)
ns
WT KO
E
Undamaged
CTX
Wild type
NELF-BscKO
1mm
Normalized TA weight (%)
**
WT KO
F
Undamaged
CTX
Wild type
NELF-BscKO
50 µm
Minimal Feret Diameter (µm)
****
WT KO WT KO
Control CTX

Figure S1 (Related to Figure 1). Loss of NELF results in decreased myofiber diameter but not myofiber numbers. A) Schematic representation of muscle regeneration. Skeletal muscle regeneration requires MuSCs to transition through 4 different states, namely quiescent MuSCs (green), activated MuSCs (red), proliferating myoblasts (blue), and multinucleated differentiated myofibers (yellow). **B)** Immunofluorescent characterization of undamaged TA muscle following long-term tamoxifen induction (8-weeks) shows no significant difference in the abundance of $Pax7^{+}$ MuSCs normalized to the amount of fibers within a field of view in NELF-B^{scKO} populations [3.96% ± 0.38, n=3] when compared to WT controls [4.20% ± 0.59, n=3]. **C)** Hematoxylin & Eosin staining on undamaged TA cross-sections from B) shows no change in TA morphology and myofiber minimal Feret's diameter in the NELF-B^{scKO} [43.48 µm ± 0.27, n=3] compared to WT controls [41.92 µm ± 0.24, n=3]. **D)** Normalized amounts of newly regenerated myofibers to the undamaged contralateral leg at 28-days post injury reveal no difference in regenerated myofiber abundance in the NELF-B^{scKO} population [84.89% ± 3.55, n=3] compared to WT controls [93.17% ± 5.29, n=3]. **E)** Hematoxylin & Eosin staining of regenerated TA at 7-days post injury shows a reduced size of the regenerating TA muscle from NELF-B^{scKO} compared to WT controls. The normalized regenerated weight to the undamaged contralateral leg is significantly reduced in the NELF-B^{scKO} [55.24% ± 2.79, n=4] compared to WT controls [74.75% ± 2.33, n=3]. **F)** Magnified images from (D) show a reduced minimal Feret's myofiber diameter in the NELF-B^{scKO} population [16.54 µm ± 0.24, n=3] compared to WT controls [25.01 µm ± 0.18, n=3].

A

FACS gating strategy from input to EdU⁺ (R5) and EdU⁻ (R7) myogenic (TdT⁺AI7⁺) population

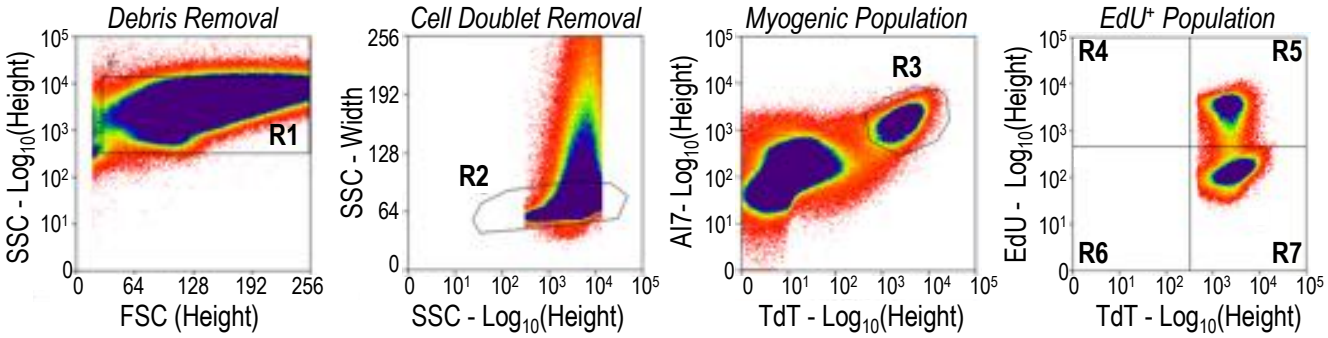

B

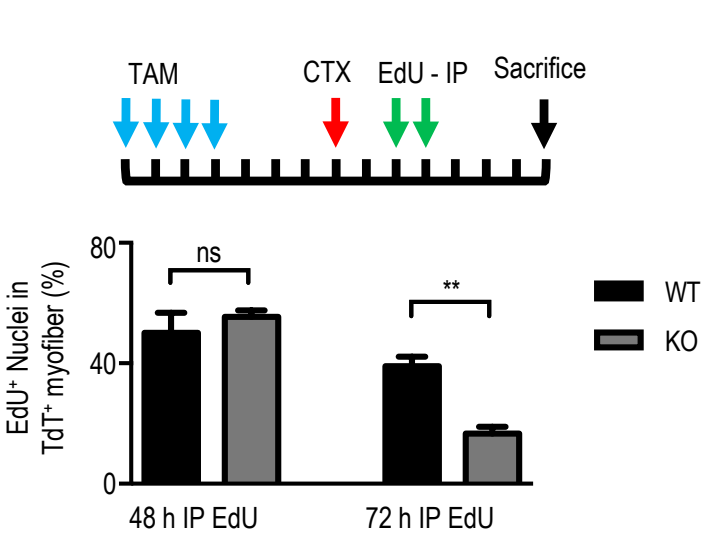

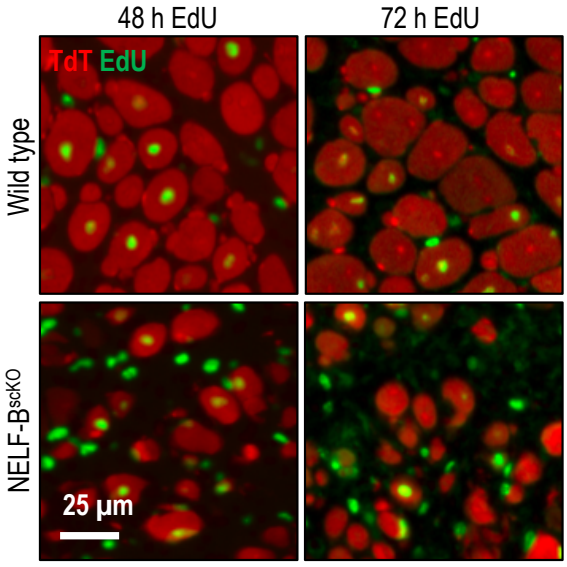

C

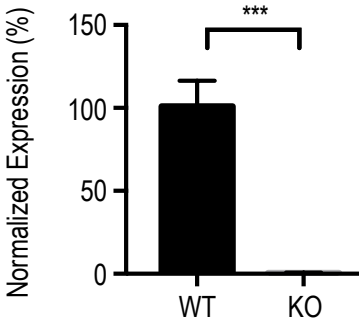

D

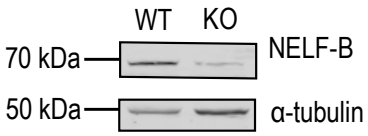

E

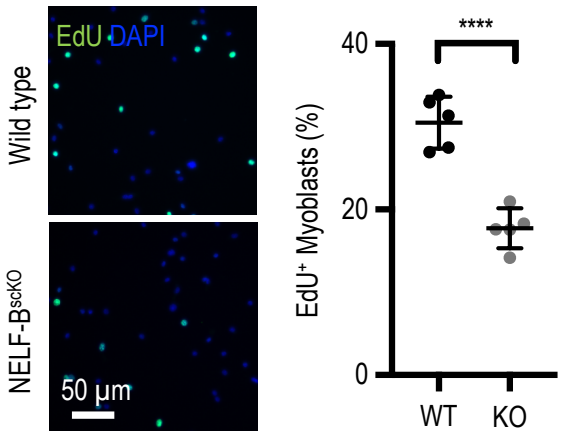

F

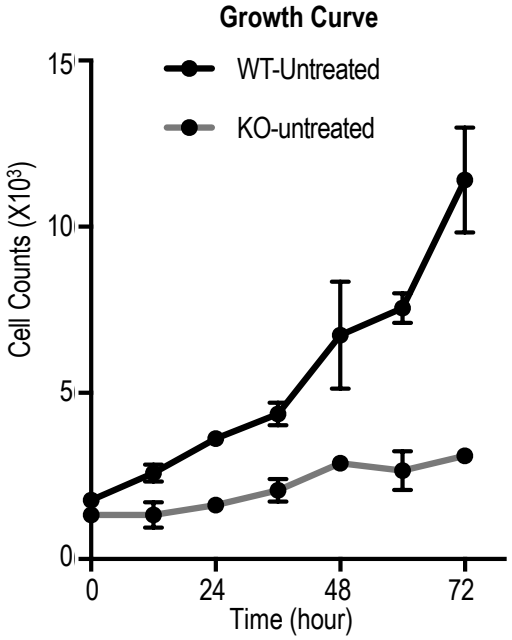

Figure S2 (Related to Figure 2). Loss of NELF impairs proliferation of muscle progenitors. **A)** FACS gating strategy applied to quantify abundance of EdU^+ MuSCs (TdT^+ $ITGA7^+$) shown in Figure 2A and 2B. First, cell debris are excluded and only cells are selected (R1); from the cell population, doublets are removed (R2) to yield only single-cell populations, which are then selected for the MuSC specific population (TdT^+ $ITGA7^+$, R3), and finally for EdU^+ populations (R5) and EdU^- populations (R7). **B)** *In vivo* EdU pulse-chase experiment administered to mice at 48-hours and 72-hour post-injury, followed with a 7-day regeneration period from time of injury. No significant difference is observed in the abundance of EdU^+ centrally-located nuclei for EdU administered at 48-hours post-injury. When EdU is administered at 72-hours post- injury, a significantly reduced amount of EdU^+ nuclei are observed in NELF-B^{scKO} [16.65% ± 2.33, n=4] mice compared to WT controls [39.01%± 3.16, n=3]. **C)** RT-qPCR quantification of *Nelfb* transcripts isolated from TdT^+ MuSCs shows that cells which are marked for recombination at the ROSA26 locus, also undergo recombination at the NELF-B locus. *Nelfb* expression levels were reduced upon tamoxifen treatment where TdT^+ MuSCs from NELF-B^{scKO} (0.56% ± 0.11, n=4) where compared to TdT^+ MuSCs from WT controls (100.90% ± 7.76, n=4). GAPDH used as an internal loading control. **D)** Western blot on whole cell extract from myoblasts induced *ex vivo* with 4-hydroxytamoxifen (4-OHT) for NELF-B^{scKO} (68kDa) and α-tubulin (50 kDa) loading control. **E**) Analysis of cell cycle progression in *ex vivo* induced myoblasts shows reduced abundance of EdU^+ myoblasts in NELF-B^{scKO} myoblasts [17.72% ± 1.08, n=5] compared to WT controls [30.50% ± 1.40, n=5]. **F)** Myoblasts from NELF-B^{scKO} and WT mice were induced with 4-OHT, then population expansion monitored at 12-hour intervals for 72 hours to monitor growth curve.

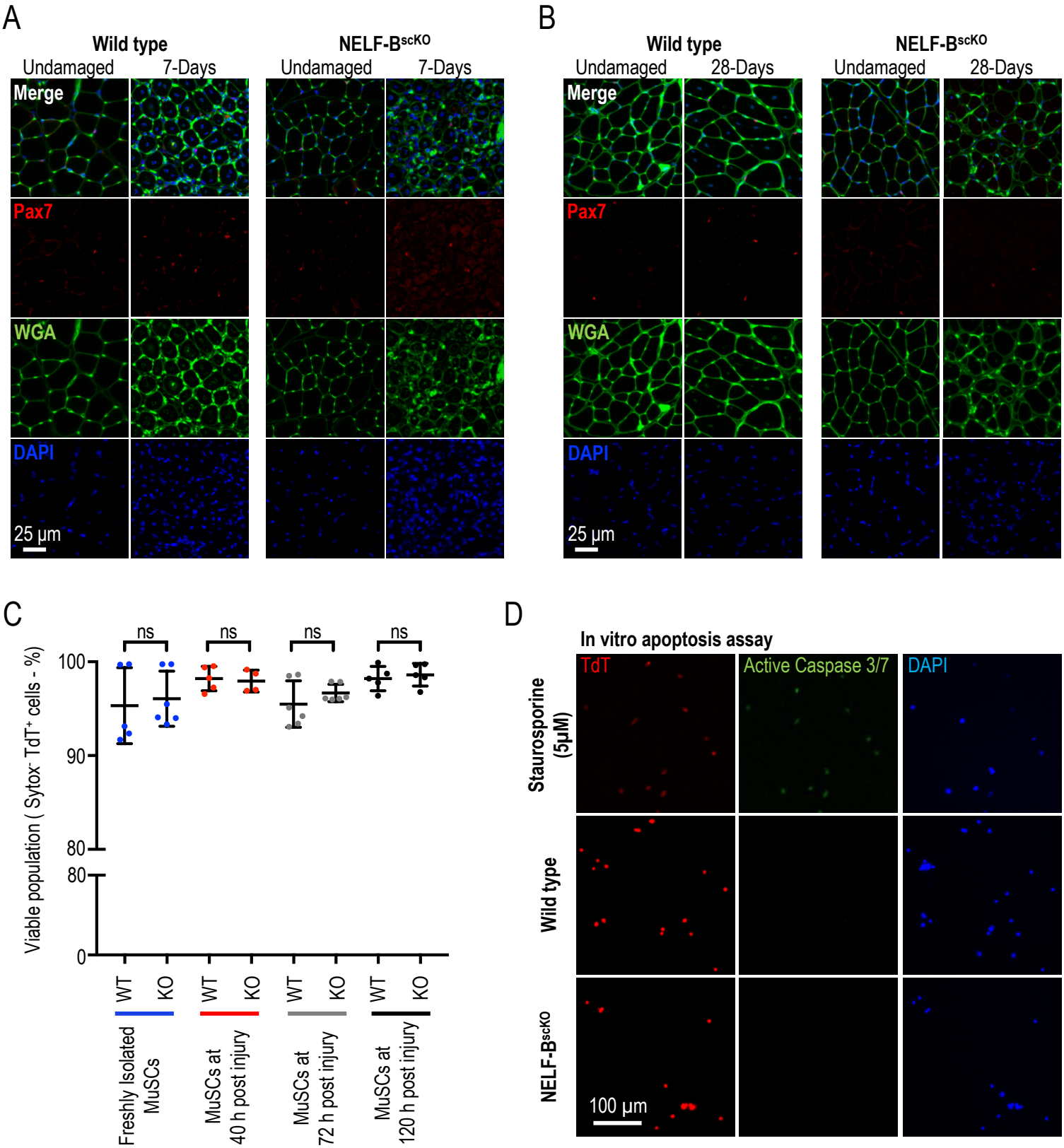
A
Wild type
NELF-BscKO
Undamaged
7-Days
Merge
Pax7
WGA
DAPI
25 µm
B
Wild type
NELF-BscKO
Undamaged
28-Days
Merge
Pax7
WGA
DAPI
25 µm
C
Viable population (Sytox- TdT+ cells - %)
100
90
80
80
0
ns
WT
KO
Freshly Isolated MuSCs
MuSCs at 40 h post injury
MuSCs at 72 h post injury
MuSCs at 120 h post injury
D
In vitro apoptosis assay
TdT
Active Caspase 3/7
DAPI
Staurosporine (5µM)
Wild type
NELF-BscKO
100 µm

Figure S3 (Related to Figure 3). MuSC pool in contralateral leg not affected in NELF- B^{scKO} mice. WT and NELF-B^{scKO} mice were injured using CTX and allowed to regenerate for **A)** 7d or **B)** 28d. Immunofluorescence analysis of the damaged TA muscle alongside of the contralateral TA from the same mouse allows the identification of MuSCs (Pax7), glycosylated proteins (WGA), and all nuclei (DAPI). **C)** Analysis of viable (Sytox^{-}) muscle progenitor cells (TdT^{+} ITGA7^{+}) from all experiments performed did not show significant differences in viable cell populations between NELF-B^{scKO} and WT muscle progenitors. Samples included viability sorting for freshly isolated MuSCs (WT : 95.32% ± 1.81, n=5; NELF-B^{scKO} : 96.06 ± 1.2, n=6), MuSCs from skeletal muscle at 40h post-injury (WT : 98.21% ± 0.58, n=5; NELF-B^{scKO} : 97.96% ± 0.58, n=4), MuSCs from skeletal muscle at 72h post-injury (WT : 95.50% ± 1.02, n=6; NELF-B^{scKO} : 96.68 ± 0.379, n=6), and myogenic progenitors from skeletal muscle at 120h post-injury (WT : 98.21% ± 0.58, n=5; NELF-B^{scKO} : 98.61 ± 0.538, n=5). **D)** Live caspase screening apoptosis assay was performed on NELF-B^{scKO} and WT myoblasts to test whether NELF-B^{scKO} affected myoblast viability. No caspase^{+} cells were identified in either NELF-B^{scKO} or WT conditions. Positive control created by treating WT myoblasts with staurosporine (5 µM, 4 hours), showing functionality of the apoptosis screening kit.

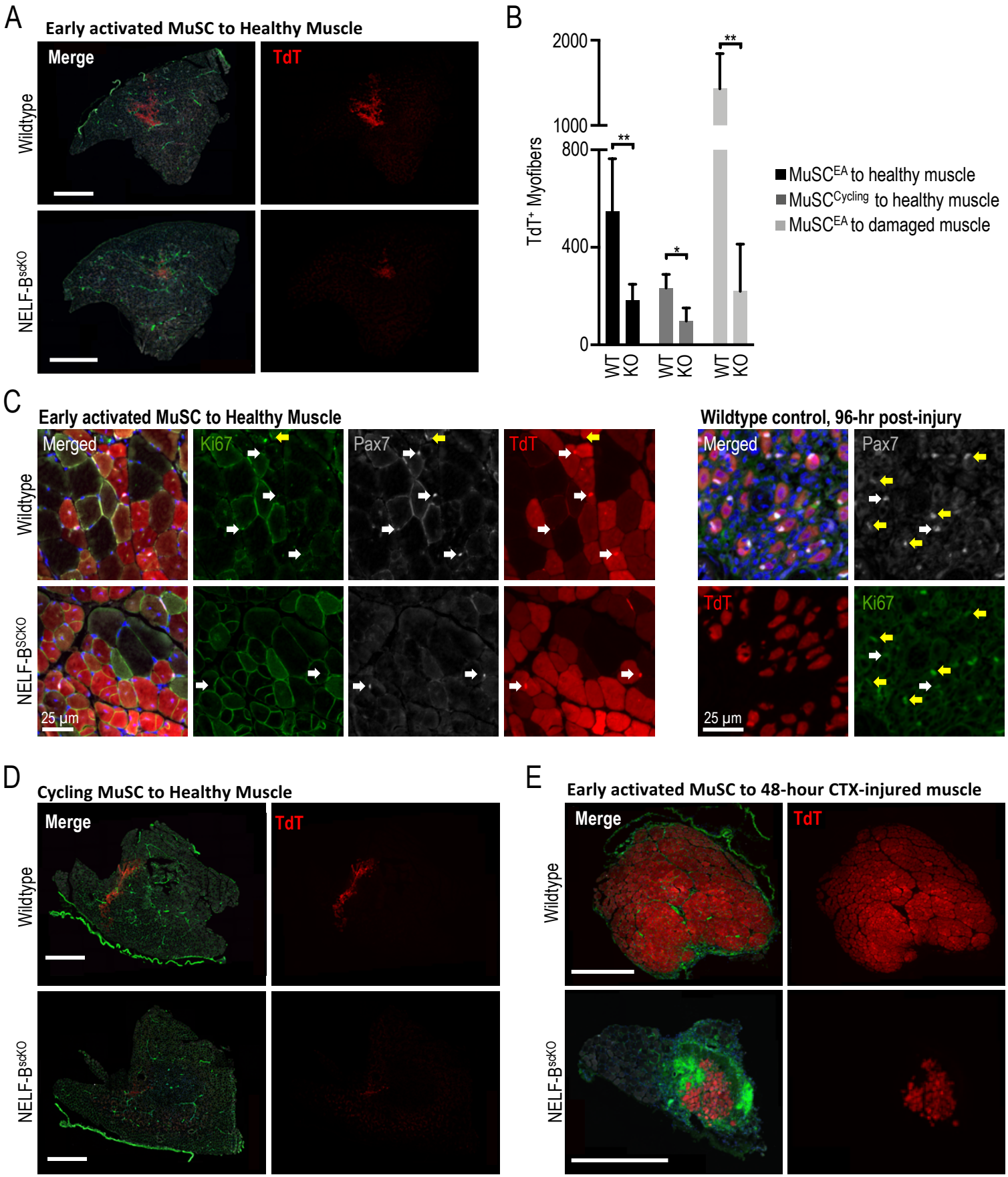
A
Early activated MuSC to Healthy Muscle
Merge
TdT
Wildtype
NELF-B scKO
B
2000
1000
800
400
0
TdT+ Myofibers
**
**
*
WT
KO
WT
KO
WT
KO
MuSC EA to healthy muscle
MuSC Cycling to healthy muscle
MuSC EA to damaged muscle
C
Early activated MuSC to Healthy Muscle
Merged
Ki67
Pax7
TdT
Wildtype
NELF-B SCKO
25 µm
Wildtype control, 96-hr post-injury
Merged
Pax7
TdT
Ki67
25 µm
D
Cycling MuSC to Healthy Muscle
Merge
TdT
Wildtype
NELF-B scKO
E
Early activated MuSC to 48-hour CTX-injured muscle
Merge
TdT
Wildtype
NELF-B scKO

Figure S4 (Related to Figure 4). Transplantation of MuSCs from NELF-B^{scKO} mice show reduced incorporation into myofibers. Immunofluorescence characterization on 10 μm cross-sections from allograft recipient mice 21-days after transplantation. In all instances, 12,000 MuSCs from NELF-B^{scKO} or WT were transplanted into irradiated NSG recipient mice. (**A**) Freshly isolated MuSCs from healthy muscle of WT and NELF-B^{scKO} donors into uninjured irradiated recipient NSG muscle. **B)** Abundance of TdT^{+} myofibers for : transplants of freshly isolated MuSCs into healthy uninjured irradiated recipient muscle shows reduced TdT^{+} myofibers upon a transplant of NELF-B^{scKO} MuSCs (181.5 ± 27.6, n=6) compared to WT (548.2 ± 96.7, n=5); reduced amount of TdT^{+} myofibers for transplant of activated MuSC from NELF-B^{scKO} (97.33 ± 31.39, n=3) compared to WT (233.2 ± 25.1, n=5), and reduced TdT^{+} myofibers for transplants of freshly isolated MuSCs into regenerating skeletal muscle at 48-hours post-injury for NELF-B^{scKO} (220.0 ± 96.7, n=4) compared to WT (1431 ± 207, n=4) counterparts. **C)** Representative images for Ki67 and Pax7 co-stain of transplanted freshly isolated MuSCs from NELF-B^{scKO} and WT mice into healthy uninjured recipient NSG muscle, with positive control performed on WT muscle collected at 96-hours post-injury. **D)** Transplant of 12,000 activated MuSCs isolated from regenerating muscle of WT and NELF-B^{scKO} donors (40h after CTX injection) into uninjured irradiated recipient NSG muscle; and (**E**) transplant of freshly isolated MuSCs from healthy muscle of WT and NELF-B^{scKO} donors into irradiated recipient muscle at 48 hours after CTX damage. All scale bars depict 500 μm.

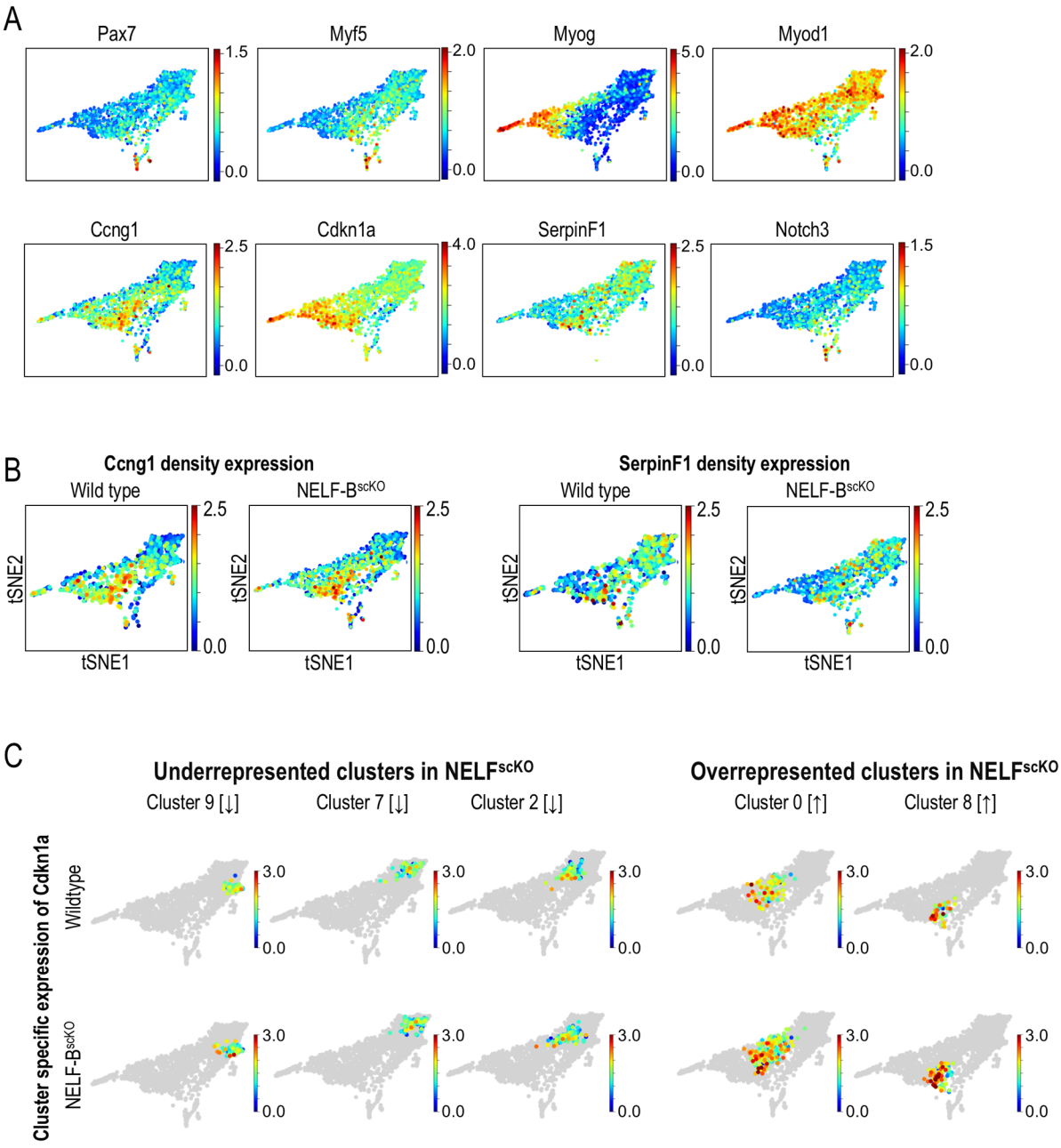
A
Pax7
1.5
0.0
Myf5
2.0
0.0
Myog
5.0
0.0
Myod1
2.0
0.0
Ccng1
2.5
0.0
Cdkn1a
4.0
0.0
SerpinF1
2.5
0.0
Notch3
1.5
0.0
B
Ccng1 density expression
Wild type
NELF-B scKO
SerpinF1 density expression
Wild type
NELF-B scKO
tSNE2
tSNE1
2.5
0.0
C
Underrepresented clusters in NELF scKO
Overrepresented clusters in NELF scKO
Cluster 9 [↓]
Cluster 7 [↓]
Cluster 2 [↓]
Cluster 0 [↑]
Cluster 8 [↑]
Cluster specific expression of Cdkn1a
Wildtype
NELF-B scKO
3.0
0.0

Figure S5 (related to Figure 5). Single-cell characterization of myogenic progenitors in skeletal muscle regeneration. A) Expression of specified myogenic regulatory factors and potential pathway-regulatory genes of interest overlaid on pseudotime PAGA trajectories (independently of genotype) . **B)** Expression of *Ccng1* and *SerpinF1* for WT and NELF-B^{scKO} showing differential expression. **C)** Expression of *Cdkn1a* over PAGA trajectory for Louvain clusters 9, 7, 2, 0, and 8 showing differential expression of the cell cycle inhibitor marker through the differentially enriched clusters.

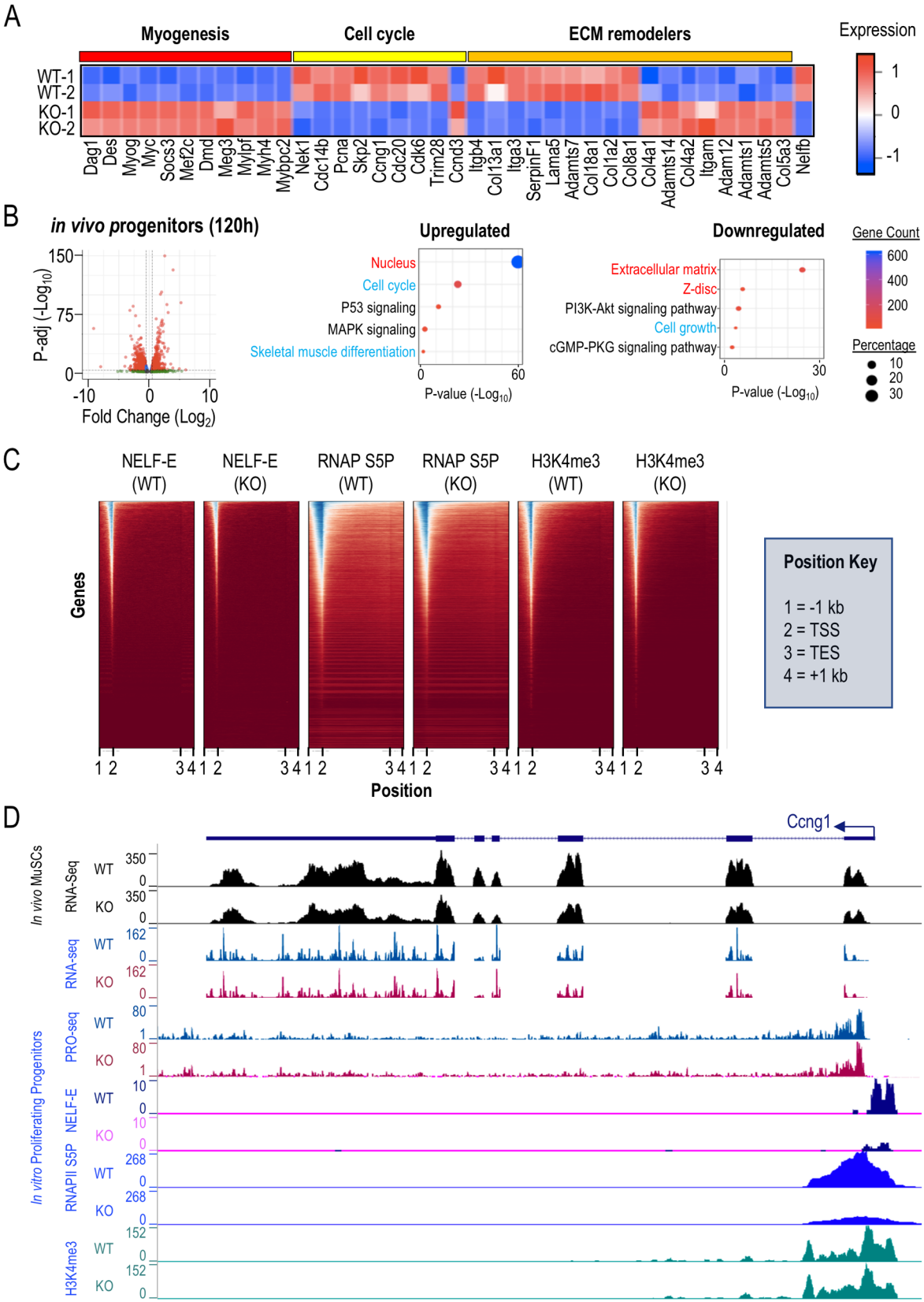
A
Myogenesis
Cell cycle
ECM remodelers
Expression
1
0
-1
WT-1
WT-2
KO-1
KO-2
Dag1 Des Myog Myc Socs3 Mef2c Dmd Meg3 Mylpf Myh4 Mybpc2 Nek1 Cdc14b Pcna Skp2 Ccng1 Cdc20 Cdk6 Trim28 Ccnd3 Itgb4 Col13a1 Itga3 SerpinF1 Lama5 Adamts7 Col18a1 Col1a2 Col8a1 Col4a1 Adamts14 Col4a2 Itgam Adam12 Adamts1 Adamts5 Col5a3 Nelfb
B
in vivo progenitors (120h)
P-adj (-Log10)
150
75
0
-10
0
10
Fold Change (Log2)
Upregulated
Nucleus
Cell cycle
P53 signaling
MAPK signaling
Skeletal muscle differentiation
0
60
P-value (-Log10)
Downregulated
Extracellular matrix
Z-disc
PI3K-Akt signaling pathway
Cell growth
cGMP-PKG signaling pathway
0
30
P-value (-Log10)
Gene Count
600
400
200
Percentage
10
20
30
C
NELF-E (WT)
NELF-E (KO)
RNAP S5P (WT)
RNAP S5P (KO)
H3K4me3 (WT)
H3K4me3 (KO)
Genes
1 2 3 4 1 2 3 4 1 2 3 4 1 2 3 4 1 2 3 4 1 2 3 4
Position
Position Key
1 = -1 kb
2 = TSS
3 = TES
4 = +1 kb
D
Ccng1
In vivo MuSCs
RNA-Seq
WT
KO
350
0
In vitro Proliferating Progenitors
RNA-seq
WT
KO
162
0
PRO-seq
WT
KO
80
1
NELF-E
WT
KO
10
0
RNAPII S5P
WT
KO
268
0
H3K4me3
WT
KO
152
0

Figure S6 (related to Figure 6). Transcriptome analysis of NELF-B^{scKO} and WT populations. **A)** Heatmap showing differential gene expression of select terms relating to myogenesis, cell cycle regulation, and ECM remodeling events on RNA-seq from myogenic progenitors captured at 48-hours post-injury. **B)** RNA-seq was performed on myogenic progenitors (TdT^{+} ITGA7^{+}) isolated from regenerating skeletal muscle at 120h post-injury, represented as a volcano plot. Gene ontology analysis performed on upregulated and downregulated terms is shown as a dotplot as a function of Log_{10}(p-value), amount of contributing terms to each GO term (dot color), and percentage of differentially expressed genes contributing to the term (dot size). **C)** Cut & Tag experiments performed for NELF-E, RNA Pol II (S5P), and H3K4me3, showing global occupancy on WT and NELF-B^{scKO} samples. *Note that tamoxifen treatment results in ~90% deletion of NELF-B in MuSCs.* **D)** Representative UCSC track for *Ccng1* shows reduced *Ccng1* expression for NELF-B^{scKO} samples compared to WT counterparts for RNA derived from MuSCs at 48h post-injury and from RNA-seq obtained from cultured myoblasts. PRO-seq analysis shows no effect on nascent transcript, while Cut & Tag experiments show reduced NELF-E and RNA Pol II (S5P) binding at the promoter region in NELF-B^{scKO} samples compared to WT counterparts.

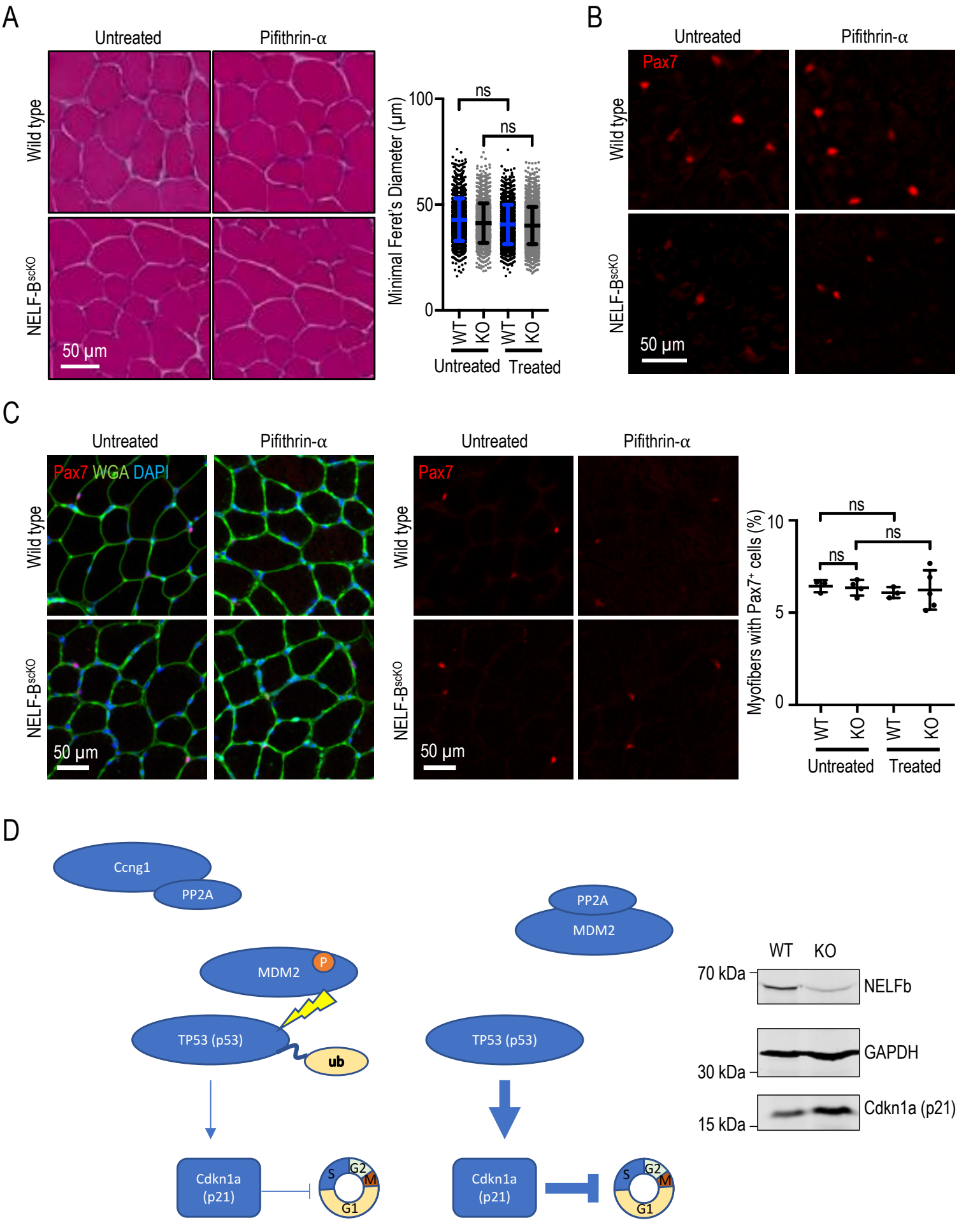
A
Untreated
Pifithrin-α
Wild type
NELF-BscKO
50 μm
Minimal Feret's Diameter (μm)
100
50
0
ns
ns
WT
KO
WT
KO
Untreated
Treated
B
Untreated
Pifithrin-α
Pax7
Wild type
NELF-BscKO
50 μm
C
Untreated
Pifithrin-α
Pax7 WGA DAPI
Wild type
NELF-BscKO
50 μm
Untreated
Pifithrin-α
Pax7
Wild type
NELF-BscKO
50 μm
Myofibers with Pax7+ cells (%)
10
5
0
ns
ns
ns
WT
KO
WT
KO
Untreated
Treated
D
Ccng1
PP2A
MDM2
P
TP53 (p53)
ub
Cdkn1a (p21)
S
G2
M
G1
PP2A
MDM2
TP53 (p53)
Cdkn1a (p21)
S
G2
M
G1
WT
KO
70 kDa
NELFb
GAPDH
30 kDa
15 kDa
Cdkn1a (p21)

Figure S7 (related to Figure 7). A) Measurements of myofiber minimal Feret's diameter from undamaged contralateral leg for WT and NELF-B^{scKO} samples in treated (pifithrin-α) and untreated conditions shows no significant difference in myofiber minimal Feret's diameter. **B)** Pax7 only field from immunofluorescent characterized regenerated TA muscle shown in Figure 7D. **C)** Immunofluorescent characterization of undamaged contralateral legs for WT and NELF-B^{scKO} 7 days after CTX damage in treated (pifithrin$-\alpha$) and untreated conditions. Abundance of Pax7^{+} cells normalized to the amount of myofibers within a field of view shows no significant difference in Pax7^{+} populations for untreated NELF-B^{scKO} (6.353 ± 0.213, n=4) to untreated WT (6.435 ± 0.191, n=3), no significant difference between Pax7^{+} cell abundance for WT-treated (6.087 ± 0.173, n=3) and WT-untreated (6.435 ± 0.1905, n=3), and no significant difference for Pax7^{+} abundance for NELF-B^{scKO} treated (6.225 ± 0.476, n=5) and NELF-B^{scKO} untreated (6.353 ± 0.213, n=4). **D)** Diagrammatic representation of regulatory pathway from Cyclin G1 to p53 regulation and effect on cell cycle. Western blot shows loss of NELF-b results in upregulation of the p53 target protein Cdkn1a (p21) in proliferating cultured myoblasts.